scientific reports

Check for updates

OPEN

ATXN3 deubiquitinates ZEB1 and facilitates epithelial–mesenchymal transition in glioblastoma

Ruting Wei[1,2,3], Xueping Shi[1,2,3], Wenjin Qiu[1], Ming Yang[1], Yimin Chen[1], Shibin Song[1], Hua Yang[1] & Jian Liu[2]✉

The activation of epithelial–mesenchymal transition (EMT) promotes glioblastoma (GBM) invasion, thereby enhancing its malignancy. Elucidating the underlying mechanisms that regulate EMT is essential for the development of effective treatments for GBM. In this study, we found that GBM tissues and cells exhibit significantly elevated expression levels of ataxin 3 (ATXN3). Functional experiments demonstrated that ATXN3 promotes the invasion, migration, and tumor growth of GBM cells by activating EMT. Mechanistically, ATXN3 was identified as a bona fide deubiquitinase for ZEB1, a key EMT-inducing transcription factor, in GBM cells. ATXN3 interacts directly with ZEB1, cleaves ubiquitin moieties from conjugated substrates and maintains the stability of ZEB1. Ectopic expression of ZEB1 significantly mitigates the inhibitory effects of ATXN3 depletion on the invasion, migration, and tumor growth of GBM cells. Furthermore, ATXN3 exhibits a positive correlation with ZEB1 expression levels and serves as a predictor of poor prognosis in human GBM specimens. Collectively, our study elucidates a critical ATXN3–ZEB1 signaling axis in EMT and invasion, thereby providing a rationale for potential therapeutic interventions against GBM.

Keywords Glioblastoma, Invasion, Migration, Deubiquitination, Protein degradation

Glioblastoma (GBM) is the most prevalent and aggressive form of primary brain tumor in adults[1,2]. The standard treatment protocol involves the maximal possible surgical resection, followed by radiation therapy and chemotherapy. Despite these interventions, the treatment's efficacy is significantly limited, and nearly all patients ultimately experience tumor recurrence after the initial therapy[3,4]. The biggest challenge in treating GBM lies in its highly invasive nature. Therefore, uncovering new mechanisms that drive GBM invasion could reveal promising molecular targets for therapeutic intervention in GBM.

Epithelial-mesenchymal transition (EMT) is a multifaceted process wherein epithelial cells undergo transdifferentiation into invasive mesenchymal cells, which plays a crucial role not only in the formation of various tissues and organs during embryogenesis but also in tumor invasion and progression[5,6]. The EMT process is typically regulated by key EMT-inducing transcription factors (EMT-TFs) such as ZEB1, ZEB2, Snail1, SLUG and Twist1. To be noted, accumulating evidence has suggested that the upregulation of EMT-TFs occurs in numerous types of tumors, thereby promoting tumor invasion and progression[5].

Deubiquitinating enzymes (DUBs) represent a vast family of proteases responsible for cleaving ubiquitin moieties from conjugated substrates, thereby inhibiting ubiquitin-dependent signaling pathways[7,8]. To date, over 100 distinct human DUBs have been identified. These DUBs are primarily classified into six major subfamilies: ovarian tumor proteases (OTUs), ubiquitin-specific proteases (USPs), ubiquitin C-terminal hydrolases (UCHs), Josephins and JAB1/MPN/MOV34 metalloenzymes (JAMM/MPN+), Machado-Joseph disease proteases (MJDs), and motif interacting with ubiquitin-containing novel DUB family (MINDYs)[9,10]. Growing evidence has demonstrated the critical role of DUBs in various cellular functions, as well as in the cancer initiation and progression[11,12]. ATXN3 is a member of JAMM/MPN+ superfamily and regulates a diverse range of biological functions such as DNA replication[13], antiviral response[14], and tumor development[15]. For example, ATXN3 has been shown to facilitate the progression of prostate cancer by deubiquitinating and stabilizing Yes-associated protein (YAP)[16]. ATXN3 also promotes breast cancer metastasis through its interaction with Krüppel-like factor 4 (KLF4), specifically by deubiquitinating and stabilizing the protein[17]. However, the function of ATXN3 in GBM has not been clarified.

[1]Department of Neurosurgery, The Affiliated Hospital of Guizhou Medical University, Guiyang 550004, Guizhou, People's Republic of China. [2]School of Clinical Medicine, Guizhou Medical University, Guiyang 550004, Guizhou, People's Republic of China. [3]Ruting Wei and Xueping Shi contributed equally to this work. ✉email: Liujian1963X@hotmail.com

In this study, we found that ATXN3 is dramatically overexpressed in human GBM tissues and cell lines. Both functional assays and animal experiments consistently showed that ATXN3 significantly promotes migration, invasion, and tumor growth by enhancing EMT in GBM cells. Additionally, we identified ATXN3 as a bona fide DUB that modulates ZEB1 polyubiquitylation and stabilization, thereby facilitating EMT and promoting invasion in GBM.

Materials and methods

Cell culture

The human glioma cell lines U251, LN229, U87MG, HS683 and SW1783 were purchased from the American Type Culture Collection and cultured in Dulbecco-modified Eagle's medium (DMEM) supplemented with 10% fetal bovine serum (FBS), glutamine, and nonessential amino acids. Normal human astrocytes (NHAs) were obtained from ScienCell Research Laboratories and maintained in astrocyte growth media supplemented with recombinant human epidermal growth factor (rhEGF), insulin, GA-1000, glutamine, ascorbic acid and 5% FBS.

Human tumor specimens

One hundred and five glioma samples (21 grades I–II, 20 grade III and 64 grade IV) and 10 normal brain tissues (NBTs) were obtained from the Department of Neurosurgery, the Affiliated Hospital of Guizhou Medical University. The histological grade of all specimens were confirmed by two independent neuro-pathologists according to the WHO criteria. This study was reviewed and approved by the Institutional Review Board and the Ethical Committee of Guizhou Medical University. Written informed consent was obtained from all patients. All experimental procedures in this study were performed in accordance with the Declaration of Helsinki.

RNA isolation and qRT-PCR

Total RNA was extracted from tissues or cells using TRIzol (Invitrogen) and the first strand cDNA was synthesized using the PrimeScript RT Master Mix (TaKaRa). Quantitative reverse transcription polymerase chain reaction (qRT-PCR) was performed according to manufacturer's protocol using SYBR Green (Applied Biosystems). Relative expression levels of target genes normalized to GAPDH were calculated using the standard $2^{-\Delta\Delta Ct}$ method. The sequences of PCR primers are as follows: ATXN3, 5′-TGACGGGTCCAGAATTAATATCA G-3′ (forward) and 5′-TGCATCTGTTGGACCCTAATCA-3′ (reverse); ZEB1, 5′-CAGCTTGATACCTGTGAA TGGG-3′ (forward) and 5′-TATCTGTGGTCGTGTGGGACT-3′ (reverse); GAPDH, 5′-CATGTTCGTCATGG GTGTGAAA-3′ (forward) and 5′-GGCATGGACTGTGGTCATGAG-3′ (reverse).

Western blotting and antibodies

Cells were harvested and lysed using RIPA buffer (50 mM Tris–HCl [pH 8.0], 150 mM NaCl, 1% NP-40, 0.5% sodium deoxycholate, 0.1% SDS, 2 mM EDTA) containing protease inhibitor and phosphatase inhibitor cocktail (Sigma-Aldrich). Cell lysates were subjected to SDS-PAGE on 8–12% gels followed by transfer onto a polyvinylidene difluoride (PVDF) membrane (Thermo Scientific). The membranes were blocked using 5% fat-free milk, incubated with primary antibodies at 4 °C overnight, washed, conjugated with secondary antibodies, and then detected with the enhanced chemiluminescence method. All blots were routinely cut and then hybridized with antibodies in our laboratory. Anti-N-cadherin, anti-E-cadherin, anti-Fibronectin and anti-GAPDH primary antibodies were obtained from Cell Signaling Technology. Anti-Twist1, anti-Vimentin, anti-Snail1, anti-Slug, anti-ZEB1, anti-ZEB2, anti-HA tag and anti-Myc tag primary antibodies were purchased from Abcam. Anti-ATXN3 antibody was purchased from Abnova. Anti-Flag tag primary antibody and HRP-conjugated secondary antibodies were obtained from Sigma-Aldrich. All experiments were performed in triplicate and repeated at least three times.

Wound healing assay

Cells transfected with the specific plasmids or shRNA were seeded in a 6-well plate at the density of 3×10^5 cells/well. An artificial wound upon monolayer cells was created using the tip of 200 μL plastic pipette. The injury area was photographed at 24 h using microscope (Olympus, Japan) and the corresponding migration index was calculated.

Transwell invasion assay

The 24-well BD Matrigel invasion chambers (BD Biosciences) were used to perform the transwell invasion assay. Briefly, 1×10^5 cells transfected with the specific plasmids or shRNA were seeded in the upper chambers with serum-free medium. 500 μL DMEM supplemented with 10% FBS was added into the lower chamber as a chemo-attractant. After incubation for 24 h, non-invading cells above the membrane were scraped off, invading cells below the membrane were fixed by 4% paraformaldehyde, stained with 0.1% crystal violet. The total number of cells adhering to the lower surface of the membrane was photographed and calculated in three representative fields. Experiments were repeated at least three times.

CCK-8 assay

Cell proliferation was detected using the CCK-8 kit (Beyotime, China) according to the manufacturer's protocol. Briefly, 2×10^3 cells transfected with the specific plasmids or shRNA were seeded in a 96-well plate, and 10 μL CCK-8 reagent was added per well at the indicated time points. The absorbance at 450 nm was measured to calculate the percentage of viable cells. Next, the absorbance at 450 nm was measured.

Transfection
Two non-overlapping lentiviral human ATXN3 shRNA sequences (shATXN3#1 sequence: 5′-CGTCGGTT GTAGGACTAAATA-3′; shATXN3#2 sequences: 5′-GCAGGGCTATTCAGCTAAGTA-3′) were cloned into pLKO.1/U6 (Addgene). Flag-tagged ATXN3 or C14A mutant, and Myc-tagged ZEB1 were cloned into indicated plasmids. Plasmids containing HA-tagged ubiquitin were supplied by Addgene. A QuikChange Mutagenesis Kit (Agilent Technologies) was employed for site-directed mutation of ATXN3. The cells were seeded on a 6-well plate and incubated for 24 h, and were used for transfection after reaching 70–80% confluence. All transfections used Lipofectamine 3000 (Invitrogen) and were performed following the manufacturer's instructions. Stable cell lines following transfection were screened by puromycin.

Immunohistochemical (IHC) staining
IHC staining was conducted to test ATXN3 and ZEB1 expression levels in human glioma specimens or NBTs as described previously[18].

Co-immunoprecipitation (Co-IP) assay
NETN buffer containing protease inhibitors was used to lyse cells subjected to different transfections. After incubation with protein A/G agarose beads (Santa Cruz) and indicated primary antibodies at 4 °C, the cell lysates were rinsed four times using NETN buffer. Immunoprecipitated complexes were then subjected to 10% SDS-PAGE gel electrophoresis and Western blotting analysis.

Ubiquitination assay
Briefly, after HA-ubiquitin transfection and 8-h treatment with MG132, cells were lysed in RIPA buffer and incubated with IgG or anti-ZEB1 antibody at 4 °C overnight. After immunoprecipitation of endogenous ZEB1 or HA-ubiquitinated Myc-ZEB1, the ubiquitination level of ZEB1 was detected by Western blotting. For in vitro ubiquitination assay, Myc-tagged ubiquitinated ZEB1 and Flag-tagged ATXN3 WT or mutant C14A were purified separately. After immunoprecipitation of HA-ubiquitinated Myc-ZEB1, the ubiquitination level of ZEB1 was detected by Western blotting.

Tumor xenograft experiment
For the tumor xenograft experiment, each 4-week-old male nude mouse (Vital River, Beijing, China) was subcutaneously injected with U251 cells (100 μL, 2×10^6) transfected with indicated plasmids (6 mice per group). Tumor volumes were calculated as $0.5 \times \text{length} \times \text{width}^2$ every ten days. After 30 days, mice were humanely euthanized with carbon dioxide, and tumors were excised and weighed. The animal care and experimental protocol were reviewed and approved by the Animal Ethics Committee and Welfare Committee of Guizhou Medical University. Additionally, the procedures adhered to the guidelines for the care and use of animals established by the National Institutes of Health Office of Laboratory Animal Welfare. This study is reported in compliance with ARRIVE guidelines.

Statistical analysis
All values are showed as mean ± standard deviation. Sample sizes and number of independent experiments were estimated by power analyses using G*Power, which takes pre-specified effect size, type I and II errors as input arguments. Shapiro–Wilk test and F test were first used to test normality and equal variance. Student's t test (two groups) or one/two-way analysis of variations (ANOVA, > two groups) were used for normal-distributed/equal variance data. A nonparametric Mann–Whitney U test was used for nonnormally distributed data. Pearson correlation was utilized to analyze the correlation between the expression levels of ATXN3 and ZEB1. The Kaplan–Meier method was used for the survival analysis of GBM patients. All data visualization and statistical analysis were performed using GraphPad Prism 9 software. $P < 0.05$ was considered statistically significant.

Results
ATXN3 expression is upregulated in GBM tissues and cell lines
Expression levels and patterns of ATXN3 in different grades of glioma specimens were first evaluated by qRT-PCR. We found that ATXN3 mRNA level significantly upregulated in high-grade gliomas compared to NBTs, especially GBM (Fig. 1A). Subsequently, we assessed the expression level of ATXN3 protein in a cohort of 105 glioma specimens, consisting of 21 grades I–II, 20 grade III, and 64 grade IV samples, as well as in 10 NBTs, utilizing western blotting and immunohistochemical analyses. Results showed that the protein level of ATXN3 was low in NBTs, but increased as glioma grade increased (Fig. 1B,C). Next, we examined the expression of ATXN3 in normal human astrocyte (NHA), three distinct subtypes of GBM cell lines U251, U87MG and LN229, and two human glioma cell lines HS683 and SW1783 (Grade III). The results suggested that ATXN3 was highly expressed in GBM cell lines but not in NHA (Fig. 1D). Taken together, these data indicated that ATXN3 was highly expressed in GBM tissues and cell lines.

ATXN3 promotes invasion and migration of GBM cells through enhancing EMT
Recent evidence has documented that ATXN3 promoted many types of malignant tumor cells migration and invasion, such as prostate cancer[16], pancreatic cancer[19], anaplastic thyroid carcinoma[20] and clear cell renal cell carcinoma[21]. It is well established that cancer cells usually acquire increased migration and invasion ability through epithelial-mesenchymal transition (EMT) process[22,23]. Given the high expression of ATXN3 in GBM tissue and cell lines, we asked whether ATXN3 is involved in the regulation of EMT, migration and invasion in GBM. To that end, we firstly knocked down ATXN3 expression in U251 and LN229 cells using green fluorescent protein-encoding short hairpin RNA (shRNA). Western blotting result confirmed that

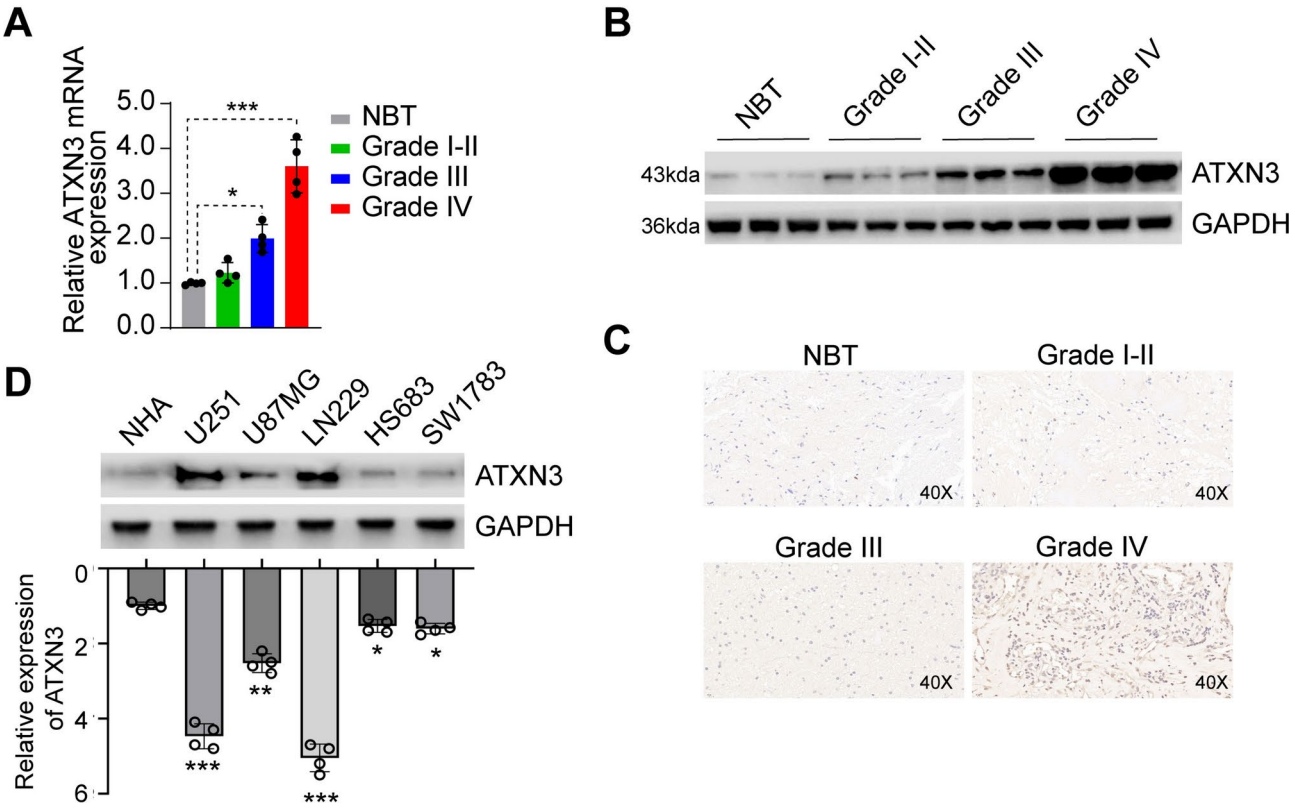

Fig. 1. ATXN3 is highly expressed in GBM tissues and cell lines. (**A,B**) The expression levels of ATXN3 mRNA (**A**) and protein (**B**) were analyzed in normal brain tissue (NBT) and gliomas tissues (grades I–IV) (*$P<0.05$, ***$P<0.001$). (**C**) The expression of ATXN3 was evaluated in NBT and glioma tissues (grades I–IV) using immunohistochemical (IHC) staining. (**D**) Western blotting analysis of ATXN3 protein levels in normal human astrocyte (NHA) and several glioma cell lines. The lower panel is quantification results (*$P<0.05$, **$P<0.01$, ***$P<0.001$).

ATXN3 protein expression significantly decreased in GBM cells transfected with ATXN3 shRNA compared to those transfected with control shRNA (Fig. 2A). Next, we tested the role of ATXN3 in GBM cells invasion and migration. The results suggested that ATXN3 depletion markedly inhibited GBM cells invasion and migration (Figs. 2B,C). In addition, we wondered whether ATXN3 also affected GBM cells proliferation. Further CCK-8 assay showed that ATXN3 inhibition significantly reduced GBM cells proliferation (Fig. 2D). The hallmark of EMT is the loss of epithelial marker expression, like E-cadherin, with a gain in mesenchymal marker expression such as of N-cadherin, Fibronectin and Vimentin[24]. Western blotting analysis showed that ATXN3 silencing remarkably elevated E-cadherin protein level, and decreased N-cadherin, Fibronectin and Vimentin protein levels (Fig. 2E). We next sought to determine whether ATXN3 overexpression affects glioma cells invasion, migration, and proliferation, we first successfully overexpressed ATXN3 in HS683 and SW1783 cells (Fig. 2F). Further cell functional experiments suggested that ATXN3 overexpression drastically promotes glioma cells invasion, migration, and proliferation (Fig. 2G–I). Furthermore, ATXN3 overexpression significantly decreased E-cadherin protein level, and upregulated N-cadherin, Fibronectin and Vimentin protein levels (Fig. 2J). Collectively, these data suggested that ATXN3 promotes invasion, migration, proliferation of GBM cells through enhancing EMT.

ATXN3 maintains the stability of ZEB1

Substantial evidence indicates that the EMT process is driven by a core set of EMT-inducing transcription factors (EMT-TFs), including ZEB1, ZEB2, Snail1, SLUG and Twist1[25–27]. To determine the impact of ATXN3 on the expression of EMT-TFs, we assessed the protein levels of EMT-TFs in ATXN3-depleted U251 and LN229 cells. Notably, among the EMT-TFs examined, only ZEB1 showed a marked reduction in after ATXN3 depletion compared to the negative control groups (Fig. 3A). Interestingly, ZEB1 mRNA expression levels were not changed while ATXN3 silencing, indicating that ATXN3 may regulate ZEB1 expression at the post-translational modification (PTMs) level (Fig. 3B). Since ATXN3 functions as a deubiquitinating enzyme (DUB), we wondered whether its regulatory effect on ZEB1 protein levels is dependent on its DUB activity. Therefore, we generated Flag-tagged ATXN3 wild-type (WT) and catalytically inactive C14A mutant plasmids and subsequently transfected them into two GBM cell lines. The results showed that ectopic expression of WT ATXN3, but not the C14A mutant, led to a significant increase in ZEB1 protein levels (Fig. 3C). Conversely, ATXN3 silencing significantly reduced ZEB1 protein levels, which could be fully reversed by the addition of the proteasome

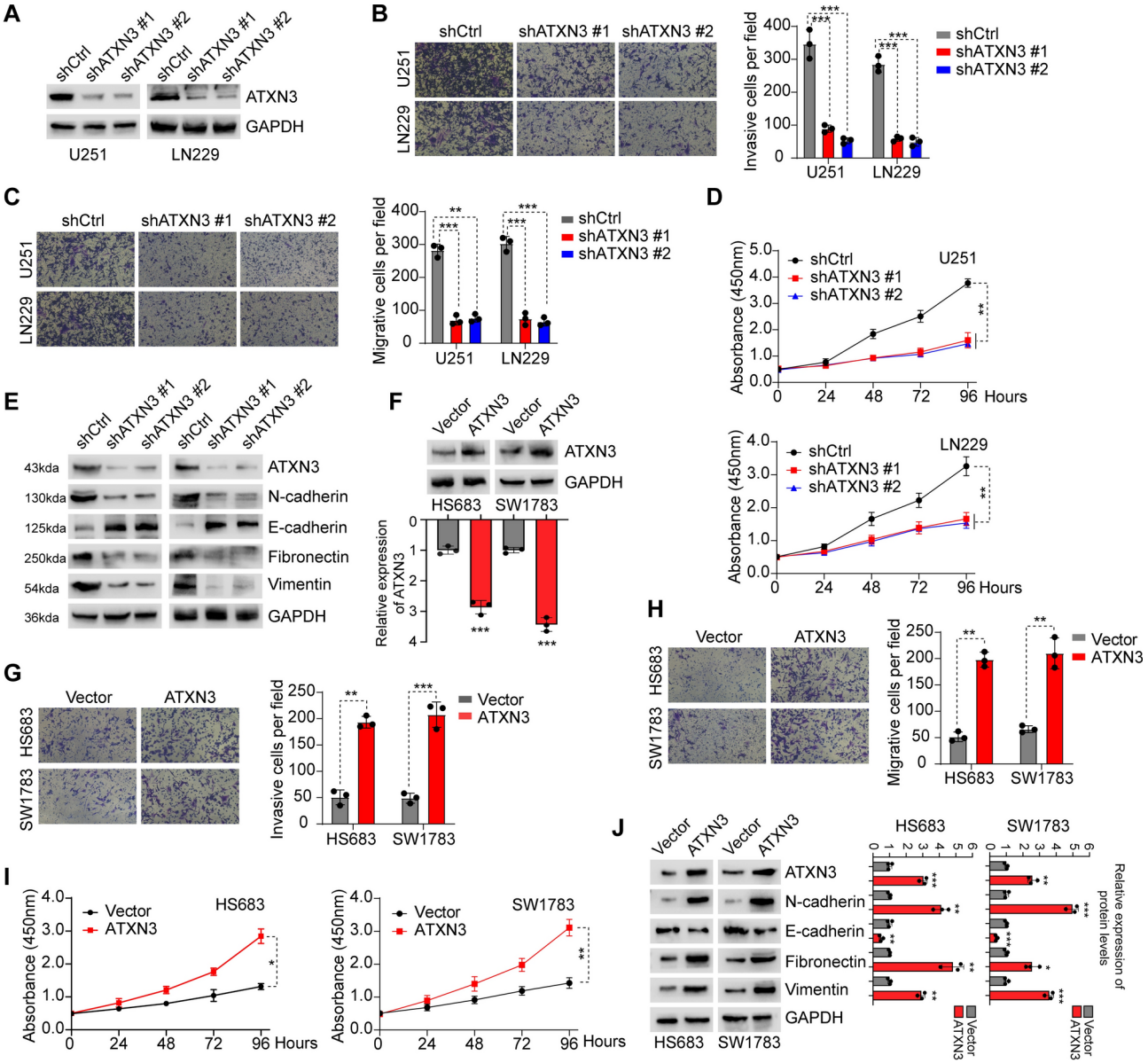

Fig. 2. ATXN3 facilitates the invasion and migration of GBM cells by promoting EMT. (**A**) Western blotting showing ATXN3 protein levels in U251 and LN229 cells transfected with two independent ATXN3-specific shRNAs (shATXN3) or a control shRNA (shCtrl). (**B,C**) Representative images of transwell invasion assay (**B**) and migration assay (**C**) using U251 and LN229 cells transfected with shATXN3#1, shATXN3#2 or shCtrl. Quantification of transwell invasion assay and migration assay are shown (**$P<0.01$, ***$P<0.001$). (**D**) CCK-8 assays showing the growth rate of 2 GBM cells after indicated treatments (**$P<0.01$). (**E**) Western blotting showing EMT-associated protein expression levels in ATXN3-depleted U251 and LN229 cells. (**F**) Western blotting showing ATXN3 protein levels in HS683 and SW1783 cells transfected with ATXN3 or vector control. The lower panel is quantification results (***$P<0.001$). (**G,H**) Representative images of transwell invasion assay (**H**) and migration assay (**G**) using HS683 and SW1783 cells transfected with ATXN3 or vector control. Quantification of transwell invasion assay and migration assay are shown (**$P<0.01$, ***$P<0.001$). (**I**) CCK-8 assays showing the growth rate of HS683 and SW1783 cells after ATXN3 overexpression (*$P<0.05$, **$P<0.01$). (**J**) Western blotting showing EMT-associated protein expression levels in ATXN3-overexpressed HS683 and SW1783 cells. The right panel is quantification results (*$P<0.05$, **$P<0.01$, ***$P<0.001$).

inhibitor MG132 (Fig. 3D). Furthermore, we assessed the degradation rate of ZEB1 protein in two GBM cell lines treated with the protein synthesis inhibitor cycloheximide. The results revealed that ATXN3 knockdown significantly increased the degradation rate of ZEB1 (Fig. 3E–H). Taken together, these results suggest that ATXN3 maintains the stability of ZEB1 in GBM cells.

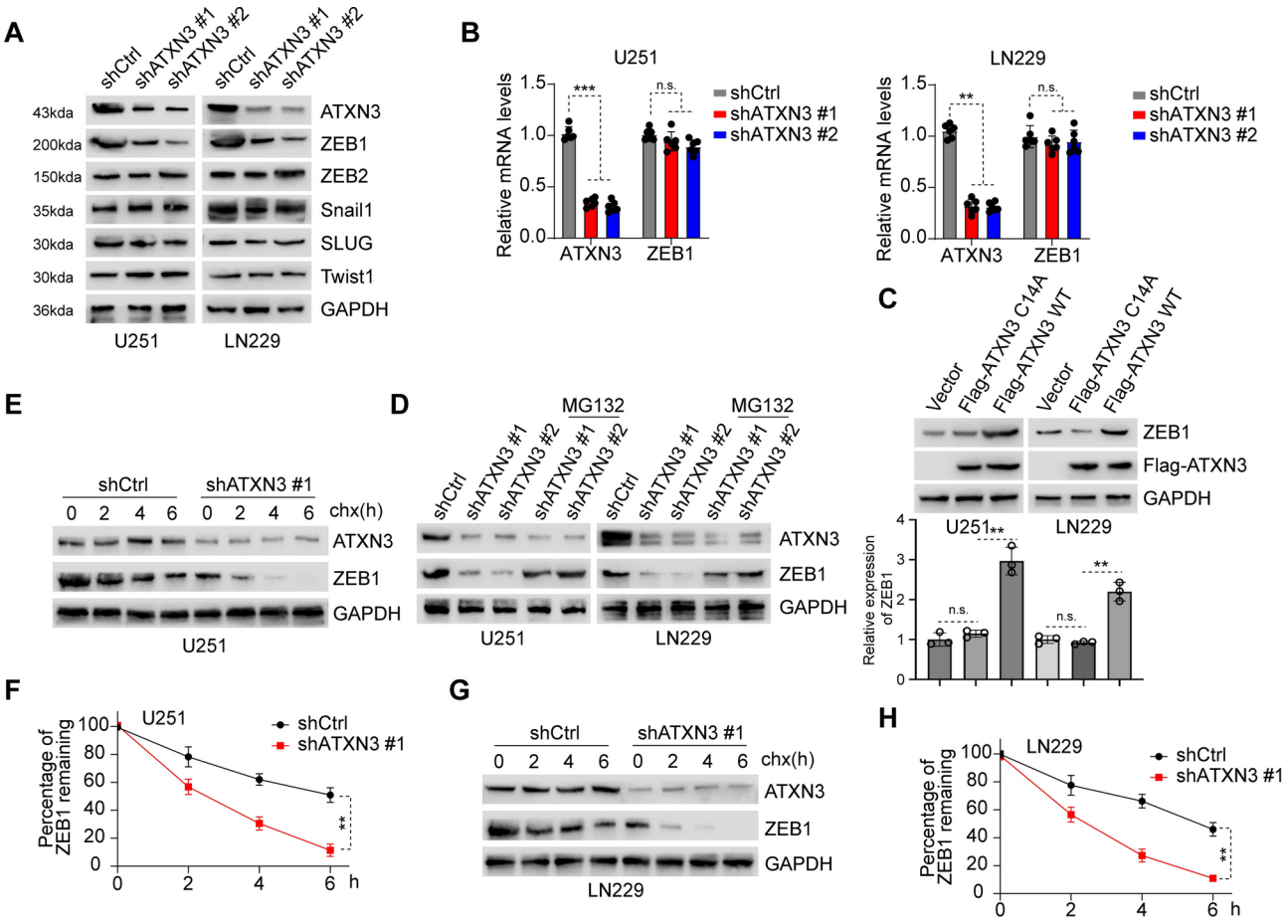

Fig. 3. ATXN3 maintains the stability of ZEB1. (**A**) Plasmids shATXN3#1, shATXN3#2 or shCtrl were stably transduced into U251 and LN229 cells. The expression levels of ATXN3, ZEB1, ZEB2, Snail1, SLUG and Twist1 were examined by western blotting using the indicated antibodies. (**B**) QRT-PCR analysis of ATXN3 and ZEB1 mRNA levels in U251 and LN229 cells transduced with shATXN3#1, shATXN3#2, or shCtrl. (**C**) Western blotting showing ZEB1 protein levels in U251 and LN229 cells transfected with Flag-tagged ATXN3 wild-type (WT) and catalytically inactive C14A mutant plasmids. The right panel is quantification results (n.s. = not significant, $^{**}P < 0.01$). (**D**) U251 and LN229 cells transduced with shATXN3#1, shATXN3#2, or shCtrl were treated with the proteasome inhibitor MG132 (20 μM, 8 h) or left untreated, followed by analysis of ATXN3 and ZEB1 protein levels. (**E–H**) U251 (**E,F**) and LN229 (**G,H**) cells transduced with shATXN3#1 or shCtrl were treated with 50 μg/ml cycloheximide for various time intervals. ZEB1 protein levels were assessed by Western blotting, and ZEB1 expression was quantified relative to GAPDH ($^{**}P < 0.01$).

ATXN3 interacts with and deubiquitinates ZEB1

To explore the interaction between ATXN3 and ZEB1, we initially co-expressed Myc-tagged ZEB1 with either Flag-tagged WT ATXN3 or the C14A mutant in HEK293T cells. Co-immunoprecipitation (Co-IP) experiments confirmed that both WT and mutant ATXN3 were capable of binding to ZEB1 (Fig. 4A). This finding indicated that the interaction between ATXN3 and ZEB1 is independent of the loss of DUB activity of ATXN3. Moreover, Co-IP assays revealed a direct physical interaction between endogenous ATXN3 and ZEB1 in two GBM cell lines (Fig. 4B). Immunofluorescence staining revealed that ATXN3 was colocalized with ZEB1 within the nuclei of U251 and LN229 cells (Fig. 4C). Together, these findings demonstrated that ATXN3 directly interacts with ZEB1. We next asked whether ATXN3 regulated ZEB1 protein level through deubiquitination. Flag-tagged WT ATXN3 or C14A mutant was first transduced into HEK293T cells and we observed that WT ATXN3, but not the C14A mutant, specifically removed ZEB1 ubiquitination (Fig. 4D). Conversely, silencing of ATXN3 by two independent shRNAs significantly increased ZEB1 polyubiquitylation in two GBM cell lines (Fig. 4E). Notably, in vitro ubiquitination assays showed that WT ATXN3, but not the mutant C14A, specifically reduces ZEB1 ubiquitination, indicating that ATXN3 was capable of directly deubiquitinating ZEB1 (Fig. 4F). These results collectively indicated that ATXN3 functions as a bona fide DUB specifically targeting ZEB1.

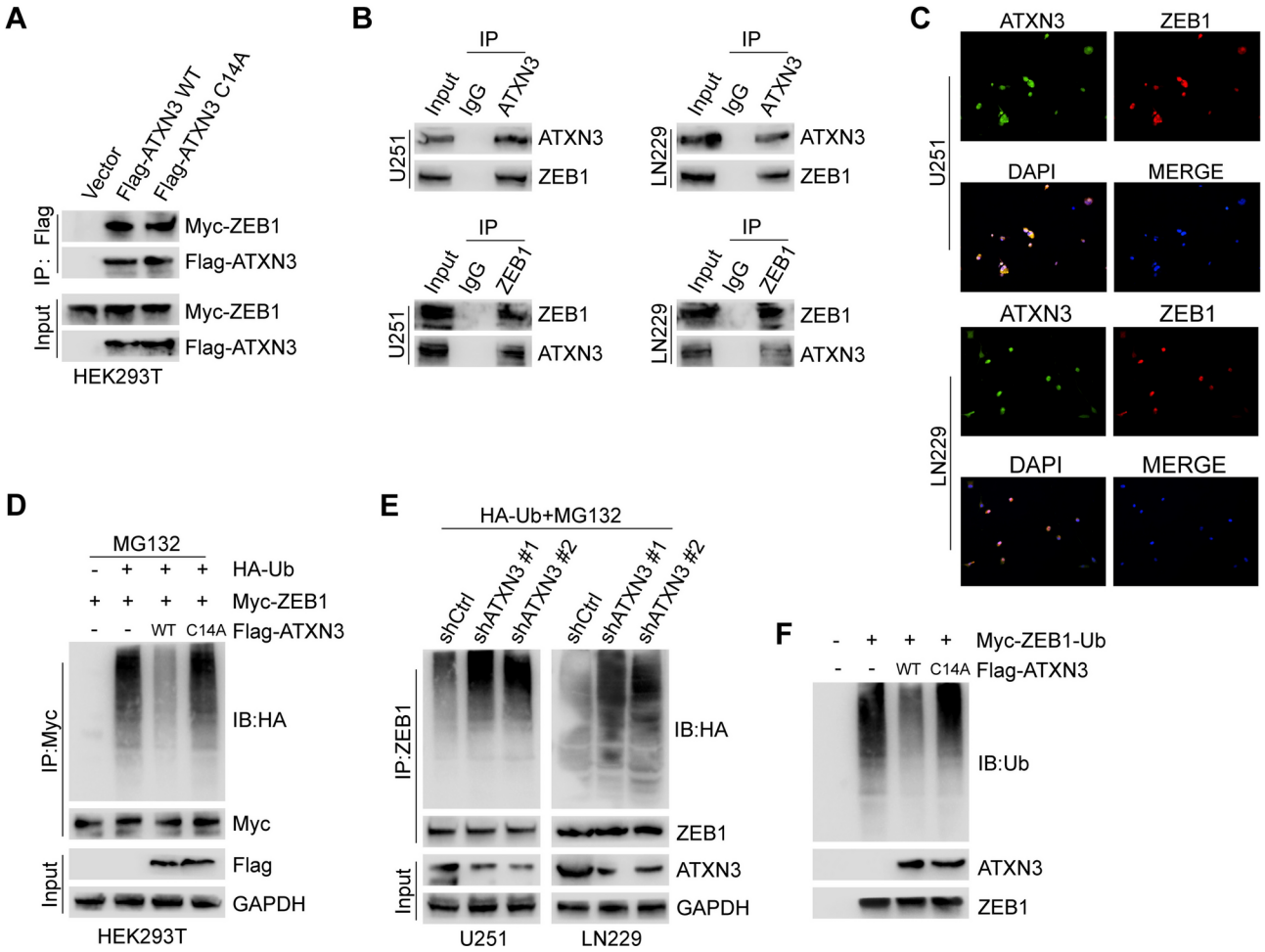

Fig. 4. ATXN3 interacts with ZEB1 and removes its ubiquitin moieties. (**A**) HEK293T cells were transduced with either Myc-ZEB1 alone or in combination with Flag-tagged ATXN3 WT or the mutant C14A. Subsequently, cell lysates were immunoprecipitated using an anti-Flag antibody, and the immunoprecipitates were analyzed by Western blotting with the specified antibodies. (**B**) Reciprocal co-immunoprecipitation of endogenous ATXN3 and ZEB1 in U251 and LN229 cells. (**C**) Representative confocal images illustrate the colocalization of ATXN3 (green) and ZEB1 (red) in U251 and LN229 cells. Scale bars = 10 μm. (**D**) Plasmids Myc-ZEB1, HA-ubiquitin (HA-Ub), and either Flag-tagged ATXN3 WT or the C14A mutant were co-transduced into MG132-treated HEK293T cells. Following this, the cells were lysed for immunoprecipitation with an anti-Myc antibody and analyzed via Western blotting. (**E**) U251 and LN229 cells transfected with HA-Ub and either shATXN3#1 or shCtrl were lysed for immunoprecipitation with an anti-ZEB1 antibody and subsequently analyzed by Western blotting. (**F**) Myc-tagged ubiquitinated ZEB1 and Flag-tagged ATXN3 WT or C14A mutant were purified from HEK293T cells. Ubiquitinated ZEB1 was then incubated with either ATXN3 WT or C14A mutant, followed by Western blotting with the indicated antibodies.

ZEB1 is essential for ATXN3-driven invasion, migration, proliferation, and tumorigenic capacity in GBM cells

Next, we aimed to evaluate the role of ZEB1 in ATXN3-mediated GBM cells invasion, migration, proliferation and tumor formation. As shown in Fig. 5A, ZEB1 overexpression completely reversed the effects of ATXN3 knockdown on the expression of N-cadherin, E-cadherin, Fibronectin, and Vimentin (Fig. 5A). Furthermore, overexpression of ZEB1 almost completely abrogated the inhibitory effects of ATXN3 silencing in GBM cells invasion, migration, and proliferation (Fig. 5B–D). Consistent with above in vitro results, ATXN3 knockdown drastically inhibited tumor formation in vivo. To be note, immune-deficient nude mice bearing ZEB1-overexpressing U251 cells, in which endogenous ATXN3 was depleted, displayed more rapid tumor growth, larger tumor volume and weight compared to the control group (Fig. 5E–G). Together, our results demonstrate that ZEB1 is a critical factor for ATXN3-induced invasive and tumorigenic properties of GBM cells.

ATXN3 is positively associated with ZEB1 protein level and predicts GBM's poor prognosis

We next tried to assess the clinical relevance of our results, the expressions of ATXN3 and ZEB1 from 64 human GBM specimens were determined using immunohistochemistry. Results showed that GBM tissue with high ATXN3 level expressed high ZEB1 level and GBM tissue with low ATXN3 level expressed low

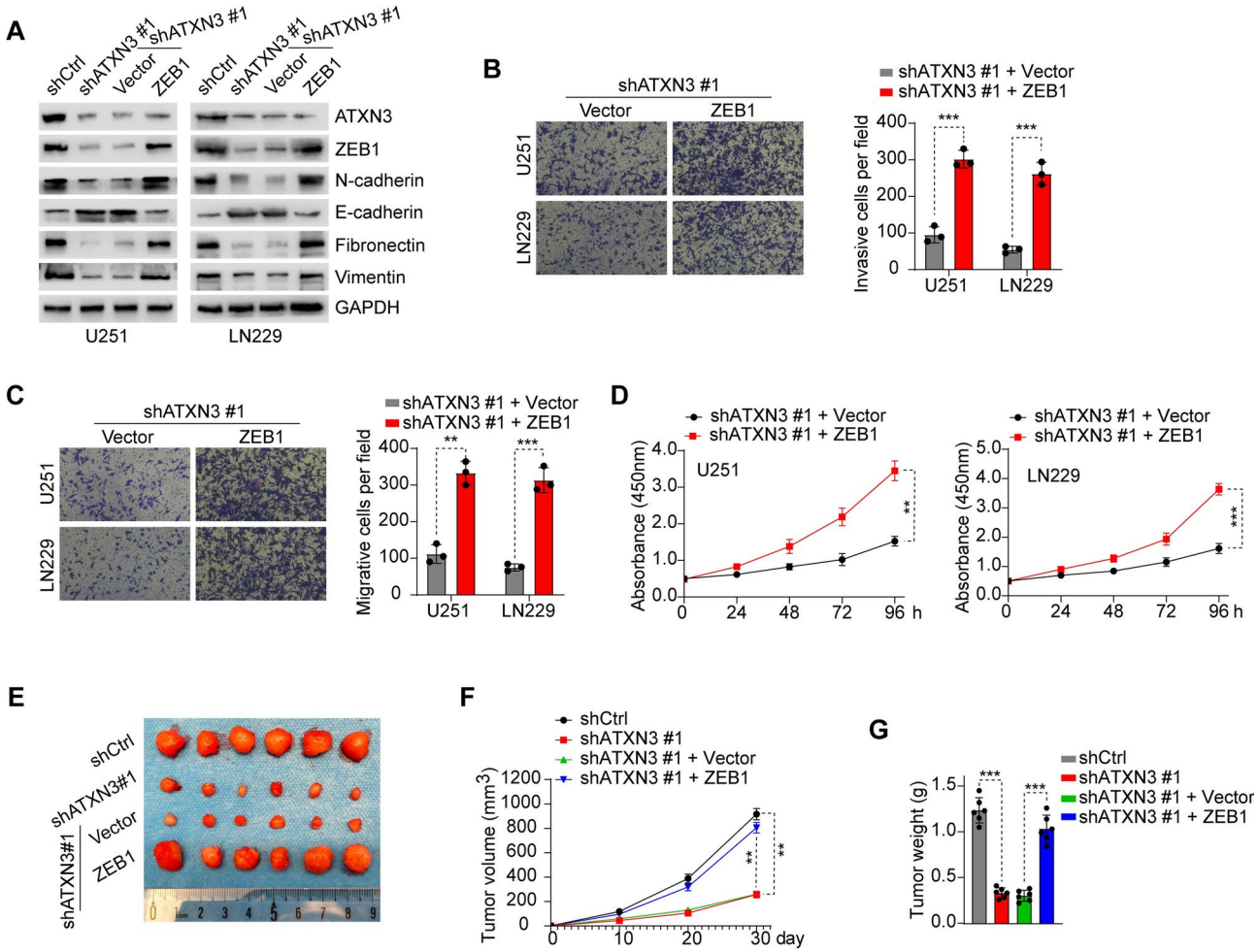

Fig. 5. ZEB1 is essential for ATXN3-driven invasion, migration, proliferation, and tumorigenic capacity in GBM cells. (**A**) Western blotting demonstrating the protein expression levels of ATXN3, ZEB1, and EMT-related proteins in U251 and LN229 cells co-transfected with shATXN3#1/shCtrl or ZEB1/vector control. B-C, Representative images of transwell invasion assay (**B**) and migration assay (**C**) in U251 and LN229 cells transfected with shATXN3#1 and either ZEB1 or empty vector. Quantification of transwell invasion assay (**B**) and migration assay (**C**) are shown (**$P < 0.01$, ***$P < 0.001$). (**D**) CCK-8 assays showing the growth rate of U251 and LN229 cells after indicated treatment (**$P < 0.01$, ***$P < 0.001$). (**E–G**) Tumor xenografts were created by subcutaneously inoculating U251 cells transfected with indicated plasmids into the right armpit of nude mice. Tumor sizes were measured every 10 days using a vernier caliper, after 30 days, the mice were sacrificed, and the tumors were excised and weighed (n = 6) (**$P < 0.01$, ***$P < 0.001$).

ZEB1 level (Fig. 6A). In addition, the results revealed a significant positive correlation between ATXN3 and ZEB1 expressions in these specimens (Fig. 6B). Kaplan–Meier survival analysis revealed that GBM patients exhibiting higher levels of ATXN3 (n = 32) experienced significantly poorer progression-free survival (PFS) and overall survival (OS) compared to those with lower ATXN3 expression (n = 32) (Fig. 6C,D). In summary, our findings indicate that ATXN3 deubiquitinates and stabilizes ZEB1, thereby facilitating EMT in GBM (Fig. 6E). Furthermore, ATXN3 shows a positive correlation with ZEB1 expression and may serve as a potential prognostic marker for GBM patients.

Discussion

Epithelial-mesenchymal transition confers more aggressive characteristics to GBM cells, which are closely associated with therapeutic resistance, tumor progression, and poor outcome. Consequently, uncovering the mechanisms driving EMT is crucial for developing more effective therapeutic strategies for GBM. In this study, we discovered that ATXN3 is significantly overexpressed in GBM and plays a crucial role in promoting GBM cell migration and invasion by facilitating EMT through stabilizing the EMT-inducing transcription factor ZEB1. Our findings revealed that ATXN3 directly interacts with ZEB1 and deubiquitinates it, thereby enhancing the invasive and tumorigenic characteristics of GBM cells.

Recent studies have reported the role of ATXN3 in various types of cancer. For instance, ATXN3 facilitated malignant progression of pancreatic cancer via deubiquitinating histone deacetylase 6 (HDAC6)[19]. ATXN3

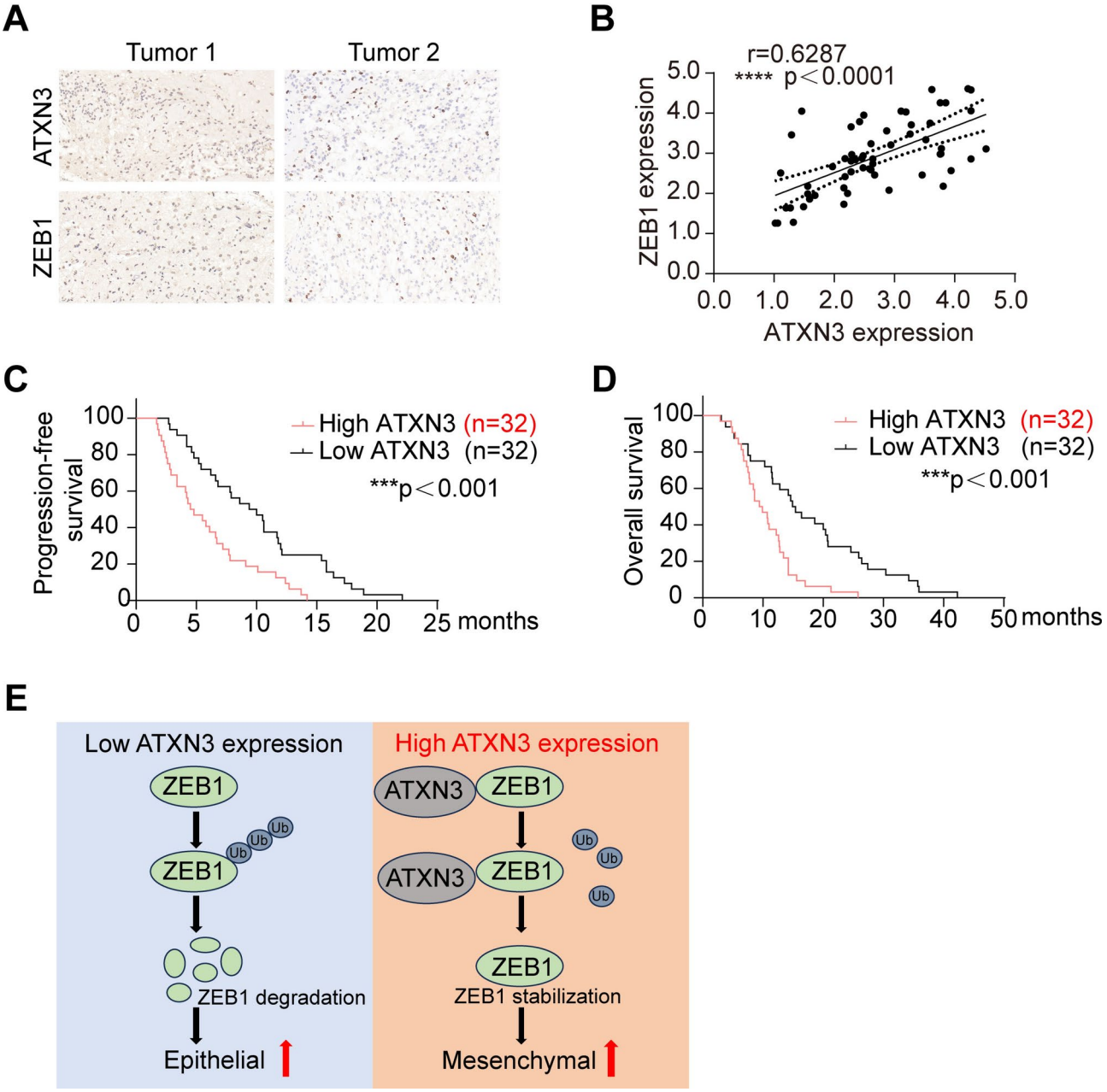

Fig. 6. ATXN3 is positively correlated with ZEB1 protein levels and serves as a predictor of poor prognosis in GBM. (**A**) Representative immunohistochemical images showing the expression levels of ATXN3 and ZEB1 in two GBM specimens. (**B**) The correlation between ATXN3 and ZEB1 expression levels was assessed using the Spearman correlation test in 64 GBM specimens. (**C,D**) Kaplan–Meier analysis of progression-free (**C**) and overall survival (**D**) in GBM patients with high (n = 32) or low (n = 32) ATXN3 expression. (**E**) Schematic illustration of the main findings of this study, which indicates that ATXN3 stabilizes ZEB1 expression and promotes EMT in GBM.

also promotes clear cell renal cell carcinoma (ccRCC) development by regulating S100A8 ubiquitination[21]. Intriguingly, a study by Cheng et al. showed that ATXN3 acts as a deubiquitinase specifically targeting galectin-9, thereby suppressing tumor development in human colon cancer[28]. Likewise, another study also supported the anti-tumor role of ATXN3 in human colon cancer[29]. These findings indicate that ATXN3 may exhibit either oncogenic or tumor-suppressive effects depending on the context within human cancers. It is worth noting that the role of ATXN3 in GBM remains largely unexplored. In the present study, we identified ATXN3 as an oncoprotein capable of promoting invasion, migration, and proliferation in GBM. Silencing ATXN3 resulted in a pronounced suppression of GBM cell invasion, migration, and proliferation. Furthermore, in vivo studies revealed that depletion of ATXN3 significantly impeded the growth of U251-derived intracranial xenografts. These findings indicate that ATXN3 holds therapeutic potential for GBM. Although effective ATXN3 antagonists

are not yet available for clinical application, our results strongly support the need for continued research and development of ATXN3-targeted therapies.

EMT is typically defined as a cellular reprogramming process in which epithelial cells undergo morphological changes, acquire increased motility, and adopt a mesenchymal phenotype[30]. This process is believed to contribute to tumor progression and metastasis, typically regulated by EMT-inducing transcription factors. ZEB1 is a critical EMT-inducing transcription factor that is strongly associated with invasion and metastasis in various types of tumors[31,32]. The ubiquitination and degradation of ZEB1 are usually regulated by a system consisting of E3 ubiquitin ligases and deubiquitinases[33]. For instance, indisulam facilitates the interaction between ZEB1 and DCAF15, a substrate receptor of the CRL4 E3 ubiquitin ligase complex, thereby enhancing the ubiquitination and proteasomal degradation of ZEB1[34]. At present, E3 ubiquitin ligases responsible for the ubiquitination of ZEB1, particularly deubiquitinases, remain inadequately explored in glioma. In the present study, our findings indicate that ATXN3 functions as a genuine DUB that specifically targets ZEB1 for deubiquitination and stabilization. It is noteworthy that our results demonstrate that the reduction in tumorigenic capacity induced by ATXN3 depletion can be largely reversed by ectopic expression of ZEB1. This finding underscores the critical role of the ATXN3/ZEB1 signaling axis in mediating the invasive and tumorigenic properties of GBM cells. We aim to investigate in future studies whether other E3 ubiquitin ligases collaborate with ATXN3 in the regulation of ZEB1 ubiquitination and degradation in glioma.

Our study has several limitations. First, we did not thoroughly explore the interplay between ATXN3 and other molecular pathways, leaving certain mechanisms unverified. Moreover, we employed subcutaneous xenografts, which do not fully replicate the brain's unique microenvironment. Consequently, future investigations using orthotopic xenograft models are essential to validate and extend our findings.

In summary, our study characterizes ATXN3 as a bona fide deubiquitinase for ZEB1, which leads to increased invasion, migration, and tumorigenic capacity of GBM cells. Targeting the ATXN3-ZEB1 signaling axis may therefore offer a novel approach for therapeutic intervention in glioblastoma.

Data availability

This research did not involve sequencing data as part of its methodology. All data generated or analyzed during this study are included in this article. Uncropped images of western blot are provided in Supplementary Document 1. Further details are available from the corresponding author upon reasonable request.

Received: 17 October 2024; Accepted: 26 February 2025
Published online: 06 March 2025

References

1. Brennan, C. W. et al. The somatic genomic landscape of glioblastoma. *Cell* **155**, 462–477 (2013).
2. Frattini, V. et al. The integrated landscape of driver genomic alterations in glioblastoma. *Nat. Genet.* **45**, 1141–1149 (2013).
3. Wen, P. Y. & Kesari, S. Malignant gliomas in adults. *N. Engl. J. Med.* **359**, 492–507 (2008).
4. Reifenberger, G., Wirsching, H. G., Knobbe-Thomsen, C. B. & Weller, M. Advances in the molecular genetics of gliomas—Implications for classification and therapy. *Nat. Rev. Clin. Oncol.* **14**, 434–452 (2017).
5. Dongre, A. & Weinberg, R. A. New insights into the mechanisms of epithelial–mesenchymal transition and implications for cancer. *Nat. Rev. Mol. Cell Biol.* **20**, 69–84 (2019).
6. Lamouille, S., Xu, J. & Derynck, R. Molecular mechanisms of epithelial–mesenchymal transition. *Nat. Rev. Mol. Cell Biol.* **15**, 178–196 (2014).
7. Komander, D., Clague, M. J. & Urbé, S. Breaking the chains: Structure and function of the deubiquitinases. *Nat. Rev. Mol. Cell Biol.* **10**, 550–563 (2009).
8. Zhou, A. et al. Gli1-induced deubiquitinase USP48 aids glioblastoma tumorigenesis by stabilizing Gli1. *EMBO Rep.* **18**, 1318–1330 (2017).
9. Kristariyanto, Y. A., Abdul Rehman, S. A., Weidlich, S., Knebel, A. & Kulathu, Y. A single MIU motif of MINDY-1 recognizes K48-linked polyubiquitin chains. *EMBO Rep.* **18**, 392–402 (2017).
10. Abdul Rehman, S. A. et al. MINDY-1 is a member of an evolutionarily conserved and structurally distinct new family of deubiquitinating enzymes. *Mol. Cell* **63**, 146–155 (2016).
11. Do, H. A. & Baek, K. H. Cellular functions regulated by deubiquitinating enzymes in neurodegenerative diseases. *Ageing Res. Rev.* **69**, 101367 (2021).
12. Ren, J. et al. Deubiquitylating enzymes in cancer and immunity. *Adv. Sci. (Weinh.)* **10**, e2303807 (2023).
13. Hernández-Carralero, E. et al. ATXN3 controls DNA replication and transcription by regulating chromatin structure. *Nucleic Acids Res.* **51**, 5396–5413 (2023).
14. Feng, Q. et al. ATXN3 positively regulates type I IFN antiviral response by deubiquitinating and stabilizing HDAC3. *J. Immunol.* **201**, 675–687 (2018).
15. Wang, S. et al. ATXN3 deubiquitinates YAP1 to promote tumor growth. *Am. J. Cancer Res.* **13**, 4222–4234 (2023).
16. Wu, L. et al. ATXN3 promotes prostate cancer progression by stabilizing YAP. *Cell Commun. Signal* **21**, 152 (2023).
17. Zou, H., Chen, H., Zhou, Z., Wan, Y. & Liu, Z. ATXN3 promotes breast cancer metastasis by deubiquitinating KLF4. *Cancer Lett.* **467**, 19–28 (2019).
18. Qiu, W. et al. USP10 deubiquitinates RUNX1 and promotes proneural-to-mesenchymal transition in glioblastoma. *Cell Death Dis.* **14**, 207 (2023).
19. Wu, X., Zhang, X., Liu, P. & Wang, Y. Involvement of Ataxin-3 (ATXN3) in the malignant progression of pancreatic cancer via deubiquitinating HDAC6. *Pancreatology* **23**, 630–641 (2023).
20. Zhuang, S. et al. The deubiquitinating enzyme ATXN3 promotes the progression of anaplastic thyroid carcinoma by stabilizing EIF5A2. *Mol. Cell Endocrinol.* **537**, 111440 (2021).
21. Bai, J., Han, J., Fan, J., Song, J. & Wang, S. ATXN3 promotes proliferation, stemness and motility of clear cell renal cell carcinoma cells by regulating S100A8 ubiquitination. *Physiol. Int.* **110**, 311–325 (2023).
22. Shenoy, A. K. & Lu, J. Cancer cells remodel themselves and vasculature to overcome the endothelial barrier. *Cancer Lett.* **380**, 534–544 (2016).
23. Makker, A. & Goel, M. M. Tumor progression, metastasis, and modulators of epithelial-mesenchymal transition in endometrioid endometrial carcinoma: An update. *Endocr. Relat. Cancer* **23**, R85–R111 (2016).

24. Cho, E. S., Kang, H. E., Kim, N. H. & Yook, J. I. Therapeutic implications of cancer epithelial–mesenchymal transition (EMT). *Arch. Pharm. Res.* **42**, 14–24 (2019).
25. Gregory, P. A. et al. The miR-200 family and miR-205 regulate epithelial to mesenchymal transition by targeting ZEB1 and SIP1. *Nat. Cell Biol.* **10**, 593–601 (2008).
26. Mani, S. A. et al. The epithelial-mesenchymal transition generates cells with properties of stem cells. *Cell* **133**, 704–715 (2008).
27. Guo, W. et al. Slug and Sox9 cooperatively determine the mammary stem cell state. *Cell* **148**, 1015–1028 (2012).
28. Cheng, Y., Wang, S., Gao, Q. & Fang, D. ATXN3 functions as a tumor suppressor through potentiating galectin-9-mediated apoptosis in human colon adenocarcinoma. *J. Biol. Chem.* **300**, 107415 (2024).
29. Li, D. et al. MicroRNA-25/ATXN3 interaction regulates human colon cancer cell growth and migration. *Mol. Med. Rep.* **19**, 4213–4221 (2019).
30. Valastyan, S. & Weinberg, R. A. Tumor metastasis: Molecular insights and evolving paradigms. *Cell* **147**, 275–292 (2011).
31. Spaderna, S. et al. The transcriptional repressor ZEB1 promotes metastasis and loss of cell polarity in cancer. *Cancer Res.* **68**, 537–544 (2008).
32. Li, L. et al. HN1L-mediated transcriptional axis AP-2γ/METTL13/TCF3-ZEB1 drives tumor growth and metastasis in hepatocellular carcinoma. *Cell Death Differ.* **26**, 2268–2283 (2019).
33. Li, X. et al. Deubiquitinase USP39 and E3 ligase TRIM26 balance the level of ZEB1 ubiquitination and thereby determine the progression of hepatocellular carcinoma. *Cell Death Differ.* **28**, 2315–2332 (2021).
34. Lu, J. et al. The aryl sulfonamide indisulam inhibits gastric cancer cell migration by promoting the ubiquitination and degradation of the transcription factor ZEB1. *J. Biol. Chem.* **299**, 103025 (2023).

Author contributions

RTW, XPS and JL conceived the project and designed the study. RTW, XPS, WJQ, and MY performed experiments. YMC and SBS collected glioma specimens. HY and RTW analyzed and interpreted the data. RTW wrote the manuscript. JL provided study supervision. All authors read and approved the final manuscript.

Funding

This work was supported by grants from the Guizhou Provincial Science and Technology Projects (Grant No. QianKeHe Foundation-ZK [2024] General-244).

Declarations

Competing interests

The authors declare no competing interests.

Ethical approval and consent to participate

This study was approved by the Institutional Review Board and the Ethical Committee of Guizhou Medical University, and performed in accordance with the Declaration of Helsinki. Written informed consent was obtained from all patients.

Additional information

Supplementary Information The online version contains supplementary material available at https://doi.org/10.1038/s41598-025-92317-w.

Correspondence and requests for materials should be addressed to J.L.